

MIT Open Access Articles

Direct Numerical Investigation of Turbulence of Capillary Waves

The MIT Faculty has made this article openly available. **Please share** how this access benefits you. Your story matters.

Citation: Pan, Yulin, and Dick K. P. Yue. "Direct Numerical Investigation of Turbulence of Capillary Waves." *Phys. Rev. Lett.* 113, 094501 (August 2014). © 2014 American Physical Society

As Published: <http://dx.doi.org/10.1103/PhysRevLett.113.094501>

Publisher: American Physical Society

Persistent URL: <http://hdl.handle.net/1721.1/89142>

Version: Author's final manuscript: final author's manuscript post peer review, without publisher's formatting or copy editing

Terms of Use: Article is made available in accordance with the publisher's policy and may be subject to US copyright law. Please refer to the publisher's site for terms of use.



Direct Numerical Investigation of Turbulence of Capillary Waves

Yulin Pan and Dick K. P. Yue

Department of Mechanical Engineering, Massachusetts Institute of Technology, Cambridge, Massachusetts 02139, USA
(Received 28 August 2013; revised manuscript received 25 July 2014; published 27 August 2014)

We consider the inertial range spectrum of capillary wave turbulence. Under the assumptions of weak turbulence, the theoretical surface elevation spectrum scales with wave number k as $I_\eta \sim k^\alpha$, where $\alpha = \alpha_0 = -19/4$, energy (density) flux P as $P^{1/2}$. The proportional factor C , known as the Kolmogorov constant, has a theoretical value of $C = C_0 = 9.85$ (we show that this value holds only after a formulation in the original derivation is corrected). The $k^{-19/4}$ scaling has been extensively, but not conclusively, tested; the $P^{1/2}$ scaling has been investigated experimentally, but until recently remains controversial, while direct confirmation of the value of C_0 remains elusive. We conduct a direct numerical investigation implementing the primitive Euler equations. For sufficiently high nonlinearity, the theoretical $k^{-19/4}$ and $P^{1/2}$ scalings as well as value of C_0 are well recovered by our numerical results. For a given number of numerical modes N , as nonlinearity decreases, the long-time spectra deviate from theoretical predictions with respect to scaling with P , with calculated values of $\alpha < \alpha_0$ and $C > C_0$, all due to finite box effect.

DOI: 10.1103/PhysRevLett.113.094501

PACS numbers: 47.27.Gs, 47.27.ek, 47.35.Pq

Introduction.—Kolmogorov [1] describes the general powerlike cascade process in the inertial range of turbulence of incompressible flow. This result has been observed in many physical systems, including plasma physics [2], capillary or gravity waves [3,4] and optics [5]. In special cases of weak (or wave) turbulence, mathematical formulations are more accessible and the cascade spectrum can be obtained as an exact stationary solution of the kinetic equation, which governs the evolution of wave spectrum due to nonlinear resonant interactions.

For capillary waves, the framework of weak turbulence theory (WTT) is developed by Zakharov and Filonenko [3] (and reformulated in [6,7]). The isotropic spectrum of surface elevation yields a powerlike solution in the inertial range which is expressed in closed form,

$$I_\eta(k) = 2\pi C \frac{P^{1/2} \rho^{1/4}}{\sigma^{3/4}} k^{-19/4}, \quad (1)$$

where C is the Kolmogorov constant with a theoretical value of $C = C_0 = 9.85$, P the energy (density) flux to large wave numbers, σ the surface tension coefficient, and ρ the fluid density. $I_\eta(k)$ is defined [6] by $\langle \hat{\eta}_{\vec{k}} \hat{\eta}_{\vec{k}'}^* \rangle = I_\eta(k) \delta(\vec{k} - \vec{k}')$, with the angle brackets denoting ensemble average and $\hat{\eta}_{\vec{k}} = 1/(2\pi) \iint_{-\infty}^{\infty} \eta_{\vec{r}} e^{-i\vec{k}\cdot\vec{r}} d\vec{r}$ being the Fourier transform of $\eta_{\vec{r}} \equiv \eta(x, y)$. In a homogeneous wave field, this definition can be shown to be equivalent to (cf. [8]) $I_\eta(k) = \iint_{-\infty}^{\infty} \langle \eta_0 \eta_{\vec{r}} \rangle e^{-i\vec{k}\cdot\vec{r}} d\vec{r}$. Due to Wiener-Khinchin theorem, $I_\eta(k)$ is proportional to the energy density spectrum $\Phi_\eta(k)$ of η [9] with a factor of $4\pi^2$.

We note that there is a difference of a factor of 2π between (1) and the form in [6]. This results from a missing factor of $1/(4\pi^2)$ in their evaluation of P , which is obtained from time derivative of energy density $E = \int S(k) d\vec{k}$,

where $S(k)$ is the spectral density of energy density. In expressing $S(k)$ in terms of wave action density and frequency, a factor of $1/(4\pi^2)$, arising as analogously between $\Phi_\eta(k)$ and $I_\eta(k)$, is missing in [6].

The spectrum (1), and especially the assumptions made in the derivation, which include phase stochasticity, infinite domain and the dominance of three-wave resonant interactions, have been the subjects of many investigations. In particular, the scaling of the spectrum with respect to wave number $I_\eta \sim k^\alpha$ has been tested experimentally [10–13] and numerically [6,14,15]. While the exponents found in [6,10,11,14,15] are consistent with the theoretical value of $\alpha_0 = -19/4$, deviations are also reported in [11,12] with $\alpha = -5.3$, and [13] with $\alpha = -6.0$ under weak or narrow-band forcing.

The scaling of I_η with P , and the value of Kolmogorov constant C , have remained open questions. Recent experimental observations from two independent groups [10,11] suggest that a linear scaling relation $I_\eta \sim P$ should apply, in apparent disagreement with (1). This controversy is summarized in [16], and appears now resolvable [17] by a better experimental estimation of P that distinguishes the energy flux from the energy dissipation at large scales. There is no direct numerical investigation of this scaling.

Attempts at estimating C numerically are given in [6] and [15] by, respectively, a potential flow simulation and a Navier-Stokes simulation, with reported values of $C_{\text{pot}} = 1.7$ and $C_{\text{NS}} = 5.0$. This value is only recently measured experimentally [17] with $C_{\text{exp}} = 0.5$. Possible reasons for these deviations from $C_0 = 9.85$ may include normalization in $I_\eta(k)$, missing 2π factor in (1), influence of gravity (for C_{exp}), and coherent structures and dissipation at broad scales (for C_{NS} and C_{exp}).

TABLE I. Maximum absolute error in surface vertical velocity $\phi_z|_\eta$ of a Crapper wave of steepness ϵ for varying nonlinearity order M and number of alias-free modes N .

ϵ	N	M				
		2	3	4	6	8
0.1	4	2.0×10^{-4}	1.1×10^{-5}	3.6×10^{-6}	2.6×10^{-6}	2.6×10^{-6}
	8	2.0×10^{-4}	1.1×10^{-5}	1.8×10^{-6}	1.7×10^{-8}	7.9×10^{-10}
	16	2.0×10^{-4}	1.1×10^{-5}	1.9×10^{-6}	1.8×10^{-8}	1.7×10^{-10}
0.2	4	1.6×10^{-3}	2.0×10^{-4}	1.1×10^{-4}	1.1×10^{-4}	1.1×10^{-4}
	8	1.6×10^{-3}	1.8×10^{-4}	6.1×10^{-5}	2.3×10^{-6}	7.3×10^{-7}
	16	1.6×10^{-3}	1.8×10^{-4}	6.1×10^{-5}	2.3×10^{-6}	9.0×10^{-8}
0.3	4	5.7×10^{-3}	1.2×10^{-3}	7.6×10^{-4}	9.4×10^{-4}	9.3×10^{-4}
	8	5.7×10^{-3}	9.6×10^{-4}	4.8×10^{-4}	4.4×10^{-5}	3.9×10^{-5}
	16	5.7×10^{-3}	9.6×10^{-4}	4.8×10^{-4}	4.2×10^{-5}	3.8×10^{-6}

Our objective is to investigate isotropic turbulence of capillary waves, and evaluate the validity of WTT, by direct numerical simulation of the primitive Euler equations. The aim is to obtain a clean development of the wave spectrum not obscured by complexities associated with the mechanical forcing of the waves [6,10,11,14,17] and difficulties associated with the estimation of P [10,11,17]. Furthermore, we seek to uncover the physics at a substantially broader range of nonlinearity level relative to existing measurements [10,11,17] and numerics [6,14,15]. To achieve this, we consider the free decay of an arbitrary initial wavefield represented by a general isotropic spectrum. We then look for the development of a powerlike spectrum in the process of freely-decaying turbulence. The energy flux P is evaluated, without ambiguity, by direct evaluation of the energy dissipation rate in the dissipation range.

We show the development of the WTT $k^{-19/4}$ powerlike spectrum, at high enough nonlinearity, with $I_\eta \sim P^{1/2}$. The Kolmogorov constant C is for the first time found to be close to C_0 (within 1% error). With decreased nonlinearity on a fixed grid (or decreased mode number N for a given nonlinearity), our results illustrate the finite box effect [6]; i.e., nonlinear resonance broadening becomes insufficient to overcome the discreteness in k , which results in a reduced energy transport. This is reflected in the reduction of P , larger and smaller values respectively of observed C and α , relative to WTT. These results offers, for the first time, both a validation of and supplement to WTT in the description of capillary wave turbulence.

Numerical formulation.—We consider capillary waves in two surface dimensions on the free surface of an ideal incompressible fluid. For small Bond number, gravity is neglected. The system is described in the context of potential flow [velocity potential $\phi(x, y, z, t)$] in terms of nonlinear evolution equations [18] for surface elevation $\eta(x, y, t)$ and velocity potential at the surface $\psi(x, y, t) \equiv \phi(x, y, \eta, t)$,

$$\eta_t = -\nabla\eta \cdot \nabla\psi + (1 + \nabla\eta \cdot \nabla\eta)\phi_z|_\eta + F^{-1}[\gamma_k\eta_k], \quad (2)$$

$$\psi_t = -\frac{1}{2}\nabla\psi \cdot \nabla\psi + \frac{1}{2}(1 + \nabla\eta \cdot \nabla\eta)\phi_z|_\eta^2 + \frac{\sigma}{\rho}\nabla \cdot \frac{\nabla\eta}{\sqrt{1 + |\nabla\eta|^2}} + F^{-1}[\gamma_k\psi_k], \quad (3)$$

where F^{-1} is the inverse Fourier transform, γ_k is the dissipation rate at small scales.

For the numerical integration of (2) and (3), we use the high-order spectral (HOS) method [19,20] (with a modification for capillarity). To verify the method's capability for modelling capillary wave, we use as a benchmark test the Crapper analytical solution for a one-dimensional capillary wave of finite amplitude [21]. Table I shows the exponential convergence of surface vertical velocity $\phi_z|_\eta$ with the nonlinearity order M and maximum wave number N (the M and N convergences are established after sufficient N and M respectively). Table II illustrates the accuracy of the method for up to $O(500)$ fundamental periods of the wave (a time scale sufficient for obtaining fully developed capillary wave spectrum).

Numerical simulation.—To model the dissipation, we introduce γ_k beyond k_γ in (2) and (3) to represent the physical (viscous) damping, with the following form in Fourier space [14]:

TABLE II. Modal error $\{1/N||\eta_{kN}|^2 - |\eta_{kA}|^2||_1\}^{1/2}/a$ (where η_{kN} and η_{kA} are the numerical and analytical solutions of η_k , and a the wave amplitude) in long time simulation of Crapper wave with $M = 3$, $N = 16$, and up to $t/T = 500$, where T is the fundamental period of the wave.

ϵ	t/T				
	100	200	300	400	500
0.3	1.9×10^{-4}	4.1×10^{-4}	5.2×10^{-4}	6.0×10^{-4}	7.4×10^{-4}

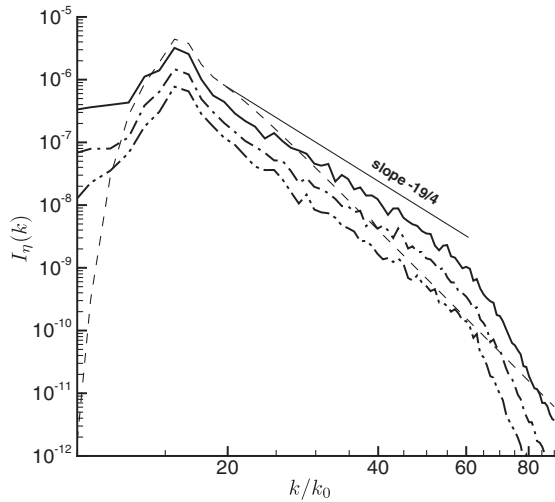


FIG. 1. Typical development of spectrum with time. Initial spectrum at $t/T_p = 0$ (dashed line), fully-developed spectrum corresponding to $\hat{P} = 9.6 \times 10^{-7}$ (solid line), decayed spectra corresponding to $\hat{P} = 1.6 \times 10^{-7}$ (single dotted dashed line) and 3.2×10^{-8} (double dotted dashed line).

$$\gamma_k = \begin{cases} \gamma_0(k - k_\gamma)^2, & k \geq k_\gamma \\ 0, & k < k_\gamma. \end{cases} \quad (4)$$

The energy (density) dissipation rate, and thus the energy (density) flux, due to (4) can be evaluated explicitly (cf. [14]):

$$P = \frac{1}{4\pi^2} \iint_{k > k_\gamma} \gamma(k) I_\psi(k) + \sigma k^2 I_\eta(k) d\vec{k}. \quad (5)$$

The simulation starts from an initial isotropic wave field with a somewhat arbitrary spectral energy distribution. The wave field is allowed to evolve freely, with total energy decreasing due to dissipation at high wave numbers. In the presence of nonlinear wave interactions, after sufficient time $t > t_A$, a powerlike spectrum develops in the inertial range. In this asymptotic phase, as the overall spectrum decays with time, its slope in the inertial range as well as scaling with P , and value of C remain quasi-stationary and are evaluated. Note that the general development of the powerlike spectrum is independent of the details of the initial spectrum (which we verify numerically). For specificity, we choose initial wave fields described by JONSWAP spectra. The nonlinearity of the initial spectrum is characterized by the effective wave steepness $\beta = k_p H_s / 2$, where k_p is the peak wave number and H_s is the significant wave height. To cover a broad range of P (and nonlinearity), we can conduct a single simulation (starting with a sufficiently large β) and follow the asymptotic spectrum as it decays. Alternatively, we can conduct different simulations with different initial spectral energies. The predicted results are effectively identical (Fig. 2).

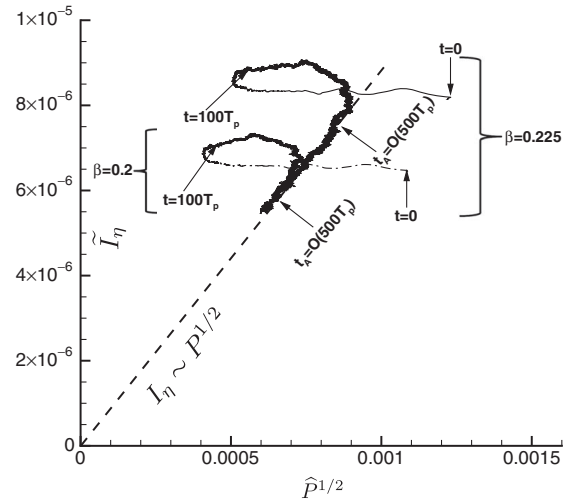


FIG. 2. Time trajectories of $(\hat{P}^{1/2}, \tilde{I}_\eta)$ for two simulations with different initial effective wave slopes: $\beta = 0.225$ (solid line) and $\beta = 0.2$ (dashed dotted line). For reference, the WTT $I_\eta \sim P^{1/2}$ scaling (dashed line) is indicated.

HOS simulations are carried out with $N_x = N_y = N = 128$ alias-free modes, with $k_p = 16k_0$ and $k_\gamma = 60k_0$, where k_0 is the fundamental wave number of the (doubly periodic) domain. For dissipation, we use $\hat{\gamma}_0 \equiv \gamma_0 k_p^2 / \omega_p = 5 \times 10^{-3}$, which obtains the asymptotic spectrum with a smooth development of and connection between the powerlike and dissipation ranges (we verify that the realized spectra and evaluation of P are not sensitive to variation of γ_0 around this choice). HOS can handle arbitrary order M of nonlinear interactions. Although the nonlinear capillary wave evolution is expected to be dominated by the three-wave process [3], we follow [14] to use $M = 3$ (corresponding to their H_2). The inclusion of four-wave processes is important for broadening the spectral tail where the nonlinearity level is low for triad resonance (cf. the discussions [6,11,14]). Thus $M = 3$ significantly speeds up the spectral evolution

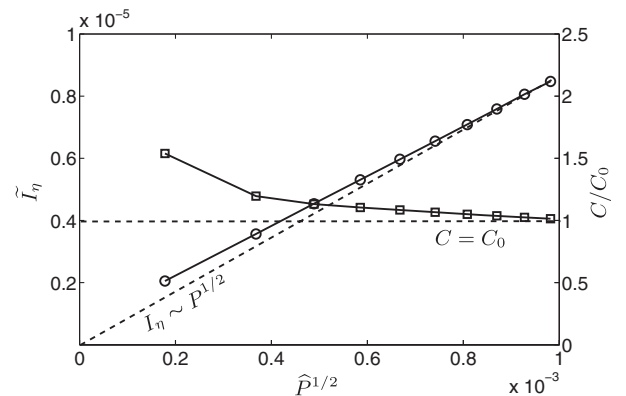


FIG. 3. \tilde{I}_η (solid line with circles) and C/C_0 (solid line with squares) as functions of $\hat{P}^{1/2}$, compared to WTT (dashed line).

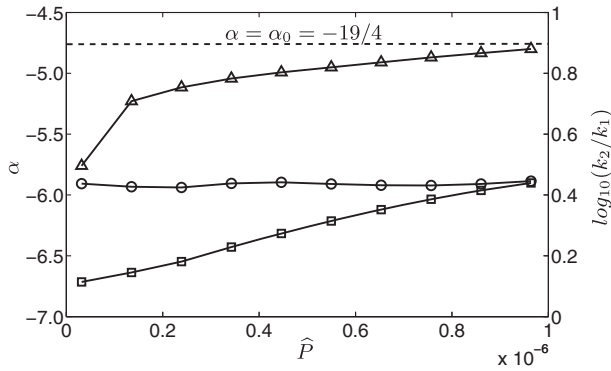


FIG. 4. Evaluated α (solid line with triangles) compared to WTT (dashed line), and $\log_{10}(k_2/k_1)_\alpha$ (solid line with circles), $\log_{10}(k_2/k_1)_{\alpha_0}$ (solid line with squares) as functions of \hat{P} .

relative to $M = 2$ (although the final predictions are little affected).

Results.—Figure 1 shows a typical evolution of the spectrum starting with $\beta = 0.25$. For this case, a powerlike spectrum is fully developed at $t_A \sim O(500T_p)$, where $T_p = 2\pi(\rho/(\sigma k_p^3))^{1/2}$. Within a substantial range, the powerlike spectrum follows closely the theoretical slope of $\alpha_0 = -19/4$. As the spectrum decays, the (normalized) energy flux $\hat{P} \equiv P/(\sigma\omega_p)$ also decreases, while the inertial range remains powerlike.

We define $\tilde{I}_\eta \equiv \int_{k_p}^{k_\gamma} I_\eta(k) dk$ as an integral measure of the amplitude of $I_\eta(k)$ within the inertial range. The time trajectories of $(\hat{P}^{1/2}, \tilde{I}_\eta)$, for two simulations with different initial values of β are plotted in Fig. 2. Indicated are the respective time t_A when the asymptotic phase is established for each case. For $t > t_A$, the slopes of the $(\hat{P}^{1/2}, \tilde{I}_\eta)$ trajectories follow closely the WTT $I_\eta \sim P^{1/2}$ scaling. We establish this scaling for a wide range of \hat{P} by repeating simulations such as those in Fig. 2 for many initial values of β or equivalently by following a long single evolution starting from large β .

Figure 3 plots $\hat{P}^{1/2}$ versus \tilde{I}_η for $\hat{P} \in [\hat{P}_{\min}, \hat{P}_{\max}]$ ranging over 1.5 decades. Our \hat{P}_{\max} is limited by the capability of HOS, and \hat{P}_{\min} is chosen to be sufficiently small to reveal the mechanism at low nonlinearity level. The WTT $P^{1/2}$ scaling is realized, with the deviation from the theoretical fit greater at lower values of \hat{P} (and \tilde{I}_η). These deviations are due to the finite box effect [6]; i.e., nonlinear resonance is limited by the finite wave number spacing. As a result, fewer triads are active in transferring energy, resulting in a reduced \hat{P} . For given N , as nonlinearity further decreases below some critical value, frozen turbulence [6] obtains and $\hat{P} \rightarrow 0$ with a finite \tilde{I}_η . The present result provides a direct numerical confirmation of $I_\eta \sim P^{1/2}$ for the first time. They thus help support the recent clarification [17] of apparent inconsistencies in the experimental predictions [10,11] and illustrate the finite box effect by substantially extending the range of \hat{P} realized in the measurements.

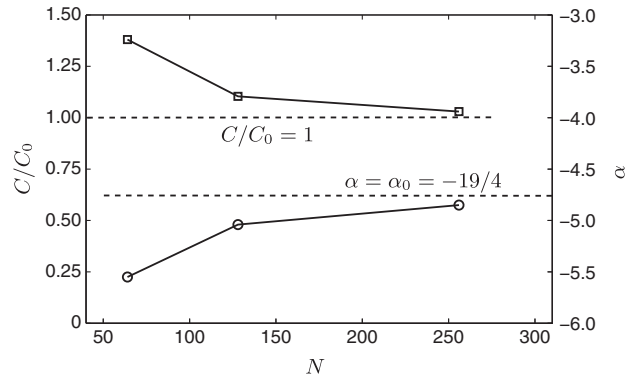


FIG. 5. C/C_0 (solid line with squares) and α (solid line with circles) compared to WTT (dashed line) with varying mode number N , for $\hat{P} = 3.4 \times 10^{-7}$.

The Kolmogorov constant C can be evaluated directly from the simulation data. Specifically, at each value of \hat{P} , we define $\kappa(\alpha) = [k_1, k_2]_\alpha$ as the maximum spectral interval within which the linear fit $\log I_\eta(k) \sim \alpha \log k$ has $R^2 > 0.99$. $C(\hat{P})$ (Fig. 3) is then evaluated from (1) in the range $\kappa(\alpha_0 = -19/4)$. The higher values of C at lower values of \hat{P} reflect the deviation from the WTT $I_\eta \sim P^{1/2}$ scaling in this range. With the increase of nonlinearity, $C(\hat{P})$ asymptotically approaches $C = 9.90$, within 1% error of the theoretical $C_0 = 9.85$.

In practice, the finite box effect, in limiting the nonlinear resonance, also results in a deviation of α from α_0 . To show this effect, at each \hat{P} , we calculate a best-fit α and the spectral range $\kappa(\alpha)$. The dependence of α on \hat{P} is shown in Fig. 4. Near \hat{P}_{\max} , $\alpha = -4.8$, and it decreases monotonically with decreasing \hat{P} to $\alpha = -5.8$ at \hat{P}_{\min} . Similar phenomenon of steepening of the spectrum at low nonlinearity has been reported in experiment for gravity wave [22]. Also reported in Fig. 4 are the widths of the spectral ranges $\kappa(\alpha)$ and $\kappa(\alpha_0)$ as functions of \hat{P} . $\kappa(\alpha)$ is almost constant, while $\kappa(\alpha_0)$ decreases monotonically with decreasing \hat{P} . In general $\kappa(\alpha) > \kappa(\alpha_0)$ except asymptotically at large \hat{P} . These results are in contrast to the theoretical self-similar decay [23], and are useful in the interpretation of observed deviations of α from α_0 in experiments [11–13].

For given nonlinearity, finite box effect can be mitigated by increasing N (or by increasing the physical dimension of the experimental tank). We show this by varying N with $N = 64$ and 256 from the preceding value of $N = 128$ (with k_p/k_0 and k_γ/k_0 scaled correspondingly). Figure 5 shows the calculated α and C with varying N . For sufficiently large N , α and C approach WTT values showing that earlier deviations from these asymptotic values are indeed manifestations of the finite box effect.

Conclusions.—In this Letter, we present results from direct numerical simulations of freely-decaying capillary wave turbulence. With the precisely evaluated P from the energy dissipation rate, we are able to confirm the WTT

$P^{1/2}$ scaling over a broad range of P . For sufficiently large P , the WTT $k^{-19/4}$ scaling and theoretical value of the Kolmogorov constant C are recovered to high accuracy. At lower nonlinearity, the deviations of the power-law spectral slope α and proportionality constant C from WTT are obtained and shown to be a result of finite box effect. The current work reinforces the validity of WTT as a description of capillary wave turbulence over a broad range of energy fluxes, and quantifies the deviations from WTT due to finite box effect when grid resolution or tank size is limited. We have studied the special case of capillary wave turbulence, our main findings are expected to also hold for weak turbulence in other similar physical systems.

-
- [1] A. Kolmogorov, Dokl. Akad. Nauk SSSR **30**, 9 (1941).
 [2] S. Galtier, S. Nazarenko, A. Newell, and A. Pouquet, *Astrophys. J. Lett.* **564**, L49 (2002).
 [3] V. E. Zakharov and N. N. Filonenko, *J. Appl. Mech. Tech. Phys.* **8**, 37 (1967).
 [4] V. Zakharov and N. Filonenko, Dokl. Akad. Nauk SSSR **170**, 1292 (1966).
 [5] S. Dyachenko, A. Newell, A. Pushkarev, and V. Zakharov, *Physica (Amsterdam)* **57D**, 96 (1992).
 [6] A. Pushkarev and V. Zakharov, *Physica (Amsterdam)* **135D**, 98 (2000).
 [7] M. Stiassnie, Y. Agnon, and L. Shemer, *Physica (Amsterdam)* **47D**, 341 (1991).
 [8] H. Risken, *Springer Ser. Synergetics* **18** (1989).
 [9] O. Phillips, *J. Fluid Mech.* **156**, 505 (1985).
 [10] E. Falcon, C. Laroche, and S. Fauve, *Phys. Rev. Lett.* **98**, 094503 (2007).
 [11] H. Xia, M. Shats, and H. Punzmann, *Europhys. Lett.* **91**, 14002 (2010).
 [12] W. B. Wright, R. Budakian, and S. J. Putterman, *Phys. Rev. Lett.* **76**, 4528 (1996).
 [13] M. Yu. Brazhnikov, G. V. Kolmakov, A. A. Levchenko, and L. P. Mezhov-Deglin, *Europhys. Lett.* **58**, 510 (2002).
 [14] A. N. Pushkarev and V. E. Zakharov, *Phys. Rev. Lett.* **76**, 3320 (1996).
 [15] L. Deike, D. Fuster, M. Berhanu, and E. Falcon, *Phys. Rev. Lett.* **112**, 234501 (2014).
 [16] A. C. Newell and B. Rumpf, *Annu. Rev. Fluid Mech.* **43**, 59 (2011).
 [17] L. Deike, M. Berhanu, and E. Falcon, *Phys. Rev. E* **89**, 023003 (2014).
 [18] V. E. Zakharov, *J. Appl. Mech. Tech. Phys.* **9**, 190 (1968).
 [19] D. G. Dommermuth and D. K. Yue, *J. Fluid Mech.* **184**, 267 (1987).
 [20] B. J. West, K. A. Brueckner, R. S. Janda, D. M. Milder, and R. L. Milton, *J. Geophys. Res.* **92**, 11803 (1987).
 [21] G. Crapper, *J. Fluid Mech.* **2**, 532 (1957).
 [22] P. Denissenko, S. Lukaschuk, and S. Nazarenko, *Phys. Rev. Lett.* **99**, 014501 (2007).
 [23] G. Falkovich, I. Y. Shapiro, and L. Shtilman, *Europhys. Lett.* **29**, 1 (1995).